

000 001 002 003 004 005 006 007 008 009 010 011 012 013 014 015 016 017 018 019 020 021 022 023 024 025 026 027 028 029 030 031 032 033 034 035 036 037 038 039 040 041 042 043 044 045 046 047 048 049 050 051 052 053 UNIVERSE-1: UNIFIED AUDIO-VIDEO GENERATION VIA STITCHING OF EXPERTS

005 **Anonymous authors**

006 Paper under double-blind review

ABSTRACT

We introduce **UniVerse-1**, a unified, Veo3-like model capable of simultaneously generating coordinated audio and video. To enhance training efficiency, we bypass training from scratch and instead employ a **stitching of experts (SoE)** technique. This approach deeply fuses the corresponding blocks of pre-trained video and music generation experts models, thereby fully leveraging their foundational capabilities. To ensure accurate annotations and temporal alignment for both ambient sounds and speech with video content, we developed an **online annotation pipeline** that processes the required training data and generates labels during training process. This strategy circumvents the performance degradation often caused by misalignment text-based annotations. Through the synergy of these techniques, our model, after being finetuned on approximately 7,600 hours of audio-video data, produces results with well-coordinated audio-visuals for ambient sounds generation and strong alignment for speech generation. To systematically evaluate our proposed method, we introduce **Verse-Bench**, a new benchmark dataset. In an effort to advance research in audio-video generation and to close the performance gap with state-of-the-art models such as Veo3, we will make our model and code publicly available. We hope this contribution will benefit the broader research community.

1 INTRODUCTION

The era of diffusion models (Song et al., 2020; Song & Ermon, 2020; Lipman et al., 2022) has culminated in the rise of Diffusion Transformer (DiT) architectures (Peebles & Xie, 2023), exemplified by landmark models like Sora (OpenAI, 2024) and its open-source counterparts (Kong et al., 2024; Yang et al., 2024; Wan et al., 2025). These models, leveraging unprecedented scales of data and computation, have achieved remarkable quality and prompt alignment in video generation. This success is catalyzing a profound transformation across creative industries and has spurred a wave of research into downstream applications such as talking head synthesis (Wang et al., 2023; Yu et al., 2023; Wang et al., 2025; Luo et al., 2025) and human animation (Tan et al., 2024; Chen et al., 2025; Lin et al., 2025), which now offer viable real-world solutions.

However, this rapid progress has been almost exclusively confined to the visual domain, treating video as a silent movie. This unimodal focus represents a fundamental bottleneck, as it ignores the inherently multimodal nature of video. Post-hoc video-to-audio models (Shan et al., 2025) serve as a superficial fix, but they are inherently limited; while capable of adapting audio to existing visual content, they fail to enforce temporal alignment in the reverse direction. This makes critical tasks, such as synchronizing lip movements with speech, impossible. While closed-source systems like Google’s Veo3 (DeepMind, 2025.5) have demonstrated synchronous audio-video generation, the lack of publicly available technical details leaves a critical gap in open research.

To bridge this gap between closed-source systems and open research, we introduce **UniVerse-1**: a unified, fully open-source, Veo3-like model capable of simultaneously generating coordinated audio and video. Our work is underpinned by several key technical contributions designed to address the unique challenges of bimodal generation.

Instead of the costly process of training a new model from scratch, we propose a novel and efficient **stitching of experts (SoE)** paradigm. This methodology effectively fuses a state-of-the-art video generation model, WAN2.1 (Wan et al., 2025), with a music generation model, Ace-step (Gong et al.,

054 2025). The core of this fusion lies in lightweight, cross-modal MLP connectors introduced within
 055 corresponding blocks of each model. These connectors facilitate bidirectional interaction between
 056 modalities, and we found this strategy to significantly accelerate training convergence by leveraging
 057 the powerful priors of the pre-trained experts.

058 Furthermore, we tackle the critical challenge of data alignment in bimodal training. We argue
 059 that static, pre-processed annotations are a flawed paradigm for tasks requiring precise temporal
 060 consistency. To address this, we developed an **online annotation pipeline** that generates labels
 061 dynamically during training. This approach ensures strict temporal and semantic alignment between
 062 audio-video data and their textual descriptions, mitigating the performance degradation caused by
 063 static misalignment. During our investigation, we also uncovered a crucial, yet overlooked, factor
 064 in bimodal diffusion modeling: **cross-modal noise correlation**. We identified that the standard
 065 pseudo-random number generation process (Hamming, 1952) can introduce spurious correlations
 066 between the noise vectors for video and audio, which subsequently degrades audio quality during
 067 inference. Our solution involves ensuring independent noise sampling for each modality.

068 To support this work, we curated a high-quality dataset comprising approximately 7,600 hours of
 069 precisely aligned audio-video content. To systematically evaluate our method, we also propose
 070 **Verse-Bench**, a new benchmark featuring 600 image-text prompt pairs covering a diverse range
 071 of sound categories. Highlighting its versatility, Verse-Bench supports not only joint audio-video
 072 generation but also unidirectional tasks, including a specialized **Verse-Ted** subset designed for
 073 evaluating audio-to-video synthesis.

074 In summary, our primary contributions are:

- 076 • **An Open-source Audio-Video Foundation Model:** We present UniVerse-1, a novel, open-source
 077 model capable of producing highly coherent and well-aligned synchronous audio-visual content,
 078 closing a critical gap in the open-source community.
- 079 • **A Novel Methodology for Joint Audio-Video Generation:** We propose a comprehensive method-
 080 ology to enable efficient and high-quality joint audio-video synthesis. This is achieved through
 081 three key innovations: a **stitching of experts (SoE)** paradigm to accelerate convergence by fusing
 082 pre-trained models; an **online data annotation pipeline** to solve the critical static misalignment
 083 problem in training (Appendix. C for more details); and the identification and mitigation of the
 084 previously overlooked **cross-modal noise correlation** issue, a crucial factor for generation quality.
- 085 • **A Comprehensive Evaluation Benchmark:** We propose Verse-Bench, a new benchmark designed
 086 to comprehensively evaluate joint audio-video generation models across a diverse set of tasks.

088 2 RELATED WORKS

090 **Video Diffusion Models** The field of video generation was revolutionized by the introduction of
 091 diffusion models, with pioneering works like AnimateDiff (Guo et al., 2023) and Video Diffusion
 092 Models (Ho et al., 2022) marking the beginning of this new era. This initial wave of research
 093 was further advanced by models such as Stable Video Diffusion (Blattmann et al., 2023), which
 094 first demonstrated that curating large-scale, high-quality datasets is critical for enhancing model
 095 performance. A common characteristic of these early models was their reliance on UNet architectures.
 096 To mitigate the challenges posed by the limited availability and quality of video data compared
 097 to images, these models were typically fine-tuned from pre-trained UNet image foundations. A
 098 significant paradigm shift occurred with the introduction of Sora (OpenAI, 2024), which heralded a
 099 new age defined by the Diffusion Transformer (DiT) architecture (Peebles & Xie, 2023) and training
 100 on massive, high-quality video corpora. This breakthrough spurred a proliferation of subsequent
 101 research. CogVideox (Yang et al., 2024) was the first to release an open-source DiT-based model,
 102 providing a significant catalyst for community-driven innovation. This was followed by other notable
 103 open-source models such as HunyuanVideo (Kong et al., 2024), WAN2.1 (Wan et al., 2025), and Step-
 104 Video (Ma et al., 2025), as well as high-performing closed-source systems including Kling (Kuaishou,
 105 2024.06), SeeDance 1.0 (Gao et al., 2025b), Movie Gen (Polyak et al., 2024), and Veo2 (DeepMind,
 106 2024.12). Architecturally, these contemporary models converge on a common blueprint. They employ
 107 a 3D Variational Autoencoder (VAE) to achieve spatio-temporal compression of video into a latent
 space. The core generative process is then handled by a DiT, which learns to denoise these noisy
 latents. Across these state-of-the-art models, the quality and scale of the training data have been

108 identified as paramount factors, making data curation and processing a central component of their
 109 development.
 110

111 **Audio Diffusion Models** The application of diffusion models to audio generation has followed
 112 a parallel trajectory to their video counterparts, fundamentally transforming the landscape of text-
 113 to-audio and text-to-music synthesis. Early explorations demonstrated the potential of diffusion
 114 for generating high-fidelity audio, but a pivotal advancement was the adoption of latent diffusion
 115 architectures (Rombach et al., 2022), which significantly improved both efficiency and quality. A
 116 common technical pipeline for these approaches involves first transforming the raw audio waveform
 117 into a mel spectrogram. A Variational Autoencoder (VAE) is then trained on this spectrogram
 118 representation to learn a compressed latent space, within which the core diffusion process operates.
 119 Within this framework, models such as Stable Audio Open (Evans et al., 2025) and Riffusion (Forsgren
 120 & Martiros., 2022) excel at generating high-fidelity, long-form audio. Furthermore, models like
 121 the AudioLDM series (Liu et al., 2024b; 2023) and DiffRhythm (Ning et al., 2025) advance these
 122 capabilities to vocal music synthesis, offering fine-grained control over rhythm and other expressive
 123 attributes.
 124

125 **Joint Audio and Video Generation** The exploration of joint audio-video generation within diffu-
 126 sion frameworks began with pioneering efforts like MM-Diffusion (Ruan et al., 2023). This model
 127 was the first to tackle this bimodal task, employing a UNet architecture with two distinct subnetworks,
 128 each dedicated to processing the audio and video modalities, respectively. Following this initial work,
 129 a series of subsequent models emerged (Ishii et al., 2024; Hayakawa et al., 2024; Ergasti et al., 2025).
 130 However, these early approaches were typically constrained by small-scale training datasets (Lee
 131 et al., 2022; Li et al., 2021), often less than 10 hours in size, which inherently limited their diversity
 132 and generalization capabilities. A notable step forward was made by models such as Syncflow (Liu
 133 et al., 2024a) and Uniform (Zhao et al., 2025), which scaled up the training data to approximately
 134 500 hours by leveraging the VGGSound (Chen et al., 2020) and AudioSet (Gemmeke et al., 2017)
 135 dataset, thereby enhancing their generalization. Despite this progress, persistent challenges remained,
 136 including suboptimal video quality and a low degree of disentanglement between the audio and
 137 visual streams. The advent of Google’s Veo3 (DeepMind, 2025.5) marked a significant milestone,
 138 representing the first large-scale initiative in synchronous audio-video generation. Veo3 demonstrated
 139 the capacity for generating high-fidelity audio and video that is not only diverse but also semantically
 140 and temporally coordinated, strictly adhering to user-provided text prompts.
 141

142 3 UNIVERSE-1

143 3.1 PRELIMINARY

144 Our model is constructed upon the foundations of the Wan2.1 (1.3B parameters) (Wan et al., 2025)
 145 text-to-video model and the Ace-step (3.5B parameters) (Gong et al., 2025) music generation model.
 146 Before delving into technical details, we will briefly introduce their respective architectures.
 147

148 **Wan2.1 model.** Wan2.1 is composed of three primary components: a 3D Variational Autoen-
 149 coder (VAE), an umT5 (Chung et al., 2023) text encoder, and a Diffusion Transformer (DiT).
 150 The 3D VAE compresses an input video of shape $(3, T, H, W)$ into a latent representation of
 151 shape $(16, T/t, H/h, W/w)$, where the temporal and spatial downsampling factors are $t = 4$ and
 152 $h = w = 8$, respectively. Prior to being input to the DiT, this latent tensor is patchified using a kernel
 153 of $(1, 2, 2)$, and the resulting tokens serve as the input sequence. The umT5 model encodes the text
 154 prompt, and its embeddings are injected into the DiT via cross-attention to condition the generation.
 155 The model is trained to predict the velocity, which is used in the denoising step to recover the clean
 156 latent. Finally, the decoder of 3D VAE reconstructs this latent into the final video.
 157

158 **Ace-step model.** Ace-step consists of a Music-DCAE (Deep Compression Autoencoder) (Chen et al.,
 159 2024), a umT5 text encoder, a lyric encoder, a speaker encoder, and a DiT. The raw audio waveform
 160 is first converted into a mel spectrogram. The Music-DCAE then encodes the input spectrogram
 161 of shape $(2, T, F)$ into a latent representation of shape $(8, T/t, F/f)$, with downsampling factors
 162 $t = f = 8$ along the temporal and frequency axes. This latent is subsequently patchified using a
 163 kernel of $(16, 1)$ to produce the input tokens for the DiT. Conditional control is provided by three
 164 sources: the umT5 encoder for the music style prompt, the lyric encoder for the lyrics, and the
 165

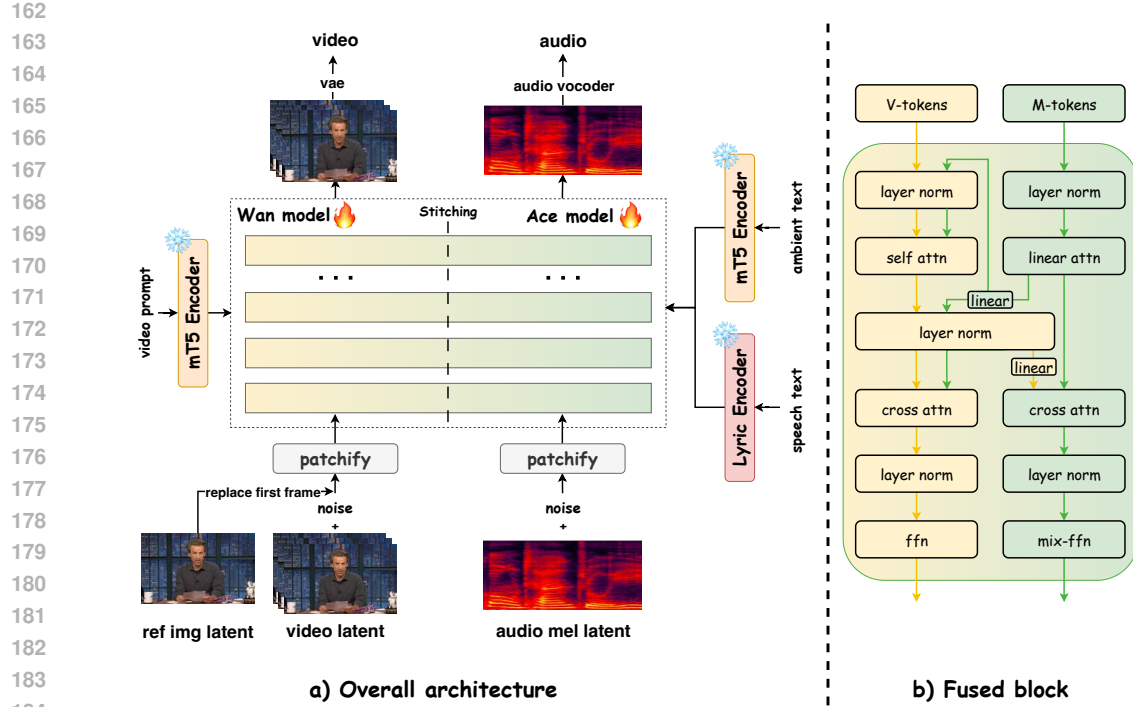


Figure 1: **Architecture of UniVerse-1.** (a) Overall architecture. The architectural foundation of UniVerse-1 is realized through a stitching of experts methodology. This approach deeply integrates the pre-trained Wan2.1 video model and the Ace-step audio model. (b) Fused block. The fusion is implemented at a granular, block-by-block level, where each block in the Wan architecture is deeply fused with its corresponding block in the Ace-step architecture.

speaker encoder for the speaker ID. These three embeddings are concatenated along the channel dimension and injected into the DiT via cross-attention. The model predicts the velocity to obtain the clean latent, which the Music-DCAE’s decoder reconstructs into a mel spectrogram. A HiFiGAN vocoder (Liao et al., 2024) is then used to convert this spectrogram into the final audio waveform.

Base model pre-training. The learning objective for both of the aforementioned models is *Flow Matching* (Lipman et al., 2022). This fashion trains a neural network, $v_\Theta(\cdot, t, c)$, to predict a velocity field that transports samples from a simple source distribution, p_0 (e.g., Gaussian noise), to a complex target data distribution, p_1 . Specifically, these models leverage Conditional Flow Matching. Given a noise sample $x_0 \sim p_0$ and a data sample $x_1 \sim p_1$, a simple linear interpolation path is defined for time t :

$$x_t = (1 - t)x_0 + tx_1. \quad (1)$$

The target velocity vector along this path is constant: $u_t = x_1 - x_0$. The model $v_\Theta(x_t, t, c)$, conditioned on c , is trained to predict this vector by minimizing the following L2 loss:

$$\mathcal{L}_{\text{FM}} = \mathbb{E}_{t \sim U(0,1), x_0 \sim p_0, x_1 \sim p_1} [\|v_\Theta((1 - t)x_0 + tx_1, t, c) - (x_1 - x_0)\|^2].$$

This objective directly trains the model to learn the vector field that maps noise to data, which leads to more stable and efficient training compared to traditional score-matching objectives.

3.2 METHOD

The overall architecture of our method is depicted in Fig. 1. We introduce several targeted modifications to the input stages of the original Wan2.1 and Ace-step models to facilitate bimodal integration and control. For the video component (Wan2.1), we enable conditioning on a reference image. During the forward process, the first frame of the noisy video latent is replaced with the corresponding clean latent representation of the provided reference image. For the audio component (Ace-step), we perform two adjustments. First, to ensure temporal alignment with the video’s 25 frames-per-second

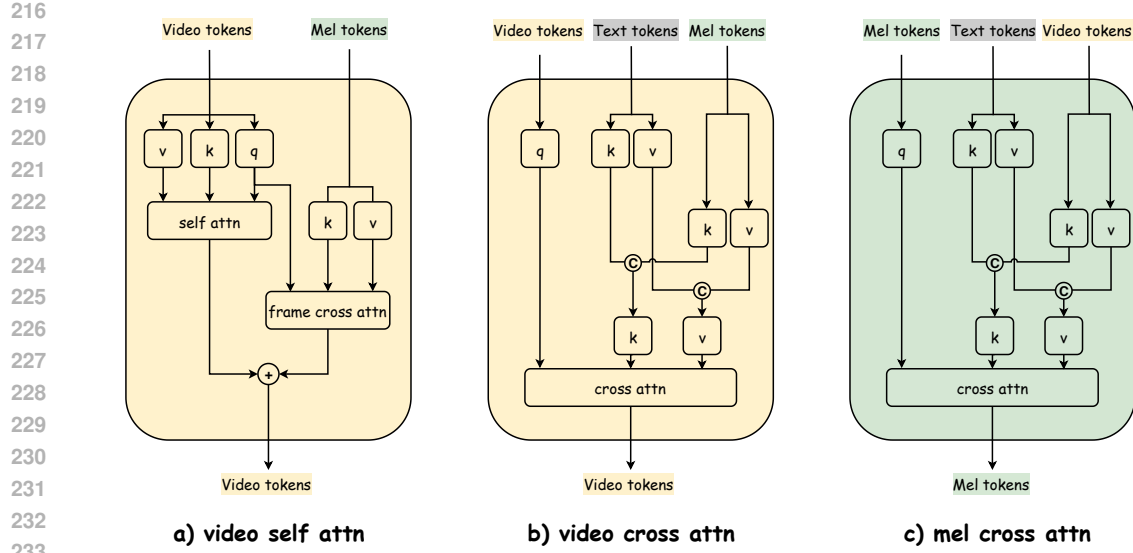


Figure 2: **Revised attention of UniVerse-1.** (a) Self attention of video branch, with additional mel tokens as input. (b) Cross attention of video branch, with additional mel tokens as input. (c) Cross attention of mel branch, with addition video tokens as input.

(fps) rate, the input mel spectrograms are processed at a 25.6 kHz sampling rate instead of the original 44.1 kHz. Second, to generalize the model beyond speaker-specific generation, we have removed the speaker encoder and its corresponding input from the architecture.

3.2.1 STITCHING OF EXPERTS

We introduce a novel framework, termed “Stitching of experts”, for integrating specialized, pre-existing models for video and audio synthesis. This approach is designed to preserve the generative capabilities of each unimodal expert while simultaneously enabling fine-grained, bidirectional interaction between them at the level of individual layer blocks. To enhance training efficiency and leverage the powerful priors of these pre-trained models, we apply the stitching technique to the Wan2.1 and Ace-step models at the transformer block level. This process results in a unified, dual-stream architecture where each block co-processes information from both the video and audio modalities, functioning akin to a Mixture-of-Experts (MoE) layer.

As illustrated in Fig 1. b), we facilitate bidirectional cross-modal communication within each block. Specifically, the hidden states from the video stream, following its self-attention module, are injected into the audio stream’s cross-attention module. Conversely, the hidden states from the audio stream, following its linear attention module, are reciprocally injected into the video stream’s self-attention and cross-attention module. To ensure consistent feature scaling, the hidden states from both streams are jointly passed through a shared LayerNorm layer before injected into video stream’s attention. Prior to injection, the cross-modal hidden states are passed through a two-layer linear adapter for feature space alignment. In the video stream, for instance, features from the audio branch are projected using dedicated key (k_{proj}) and value (v_{proj}) layers as shown in Fig. 2(a). A frame-by-frame cross-attention is then performed with the queries from the video stream to ensure alignment between the video and audio. Within each stream’s respective cross-attention mechanism(shown in Fig. 2(b) and Fig. 2(c)), the conditioning signal from the other modality is projected using dedicated key (k_{proj}) and value (v_{proj}) layers. These new key-value pairs are then concatenated with the original text-derived key-value pairs along the context dimension, thereby enriching the conditioning information with cross-modal context.

3.2.2 LAYER INTERPOLATION

A key challenge in stitching the Wan2.1 and Ace-step models is the architectural mismatch in their depth, as they possess a different number of transformer blocks. To reconcile this disparity, we

introduce a **layer interpolation technique**. This method involves first calculating the difference in the number of layers. We then strategically insert new blocks at uniform intervals into the shallower of the two models until their depths align. Crucially, the parameters for each new block are initialized by linearly interpolating the weights of its immediately adjacent (bracketing) layers. This initialization strategy effectively bridges the architectural gap while ensuring a smooth performance trajectory during training, thereby mitigating the risk of training instability and severe performance oscillations.

3.2.3 TRAINING LOSS

In addition to the primary Flow Matching objective (Sec. 3.1), we incorporate two additional loss functions.

Semantic Alignment Loss For the audio modality, we employ a **Semantic Similarity Loss** (\mathcal{L}_{SSL}), a technique consistent with Ace-step, to enhance the semantic fidelity of the generated audio. This loss operates by aligning an intermediate feature representation, h_{audio} , extracted from the audio stream of our fused block at a specific layer L ($L = 12$ in our configuration). This internal representation is aligned against target features derived from two expert, pre-trained audio models:

- **MERT**(Music Encoder Representations from Transformers) (Li et al., 2023), which provides a general musical representation, h_{mert} , with a dimensionality of $1024 \times T_m$ (at a 75 Hz frame rate).
- **mHuBERT**(multilingual HuBERT) (Boito et al., 2024), which provides a speech-centric representation, h_{mHuBERT} , with a dimensionality of $768 \times T_h$ (at a 50 Hz frame rate).

To compute this loss, the intermediate feature h_{audio} is first processed by two separate projection heads (π_{MERT} and π_{mHuBERT}) and temporally interpolated to match the dimensionality and sequence length of h_{MERT} and h_{mHuBERT} , respectively. The semantic similarity loss is then defined as the negative cosine similarity, encouraging the model’s internal representations to align with those of the expert models:

$$\mathcal{L}_{SSL} = -\frac{1}{2}(\text{cosineSim}(h'_{\text{audio}}, h'_{\text{MERT}}) + \text{cosineSim}(h'_{\text{audio}}, h'_{\text{mHuBERT}}))$$

where h' denotes the temporally aligned representations.

Low Quality Data Loss Strategy The AudioSet and VGGSound datasets, while offering rich auditory diversity, are characterized by low visual fidelity. To leverage their strong audio content without corrupting the video generation quality, we employ a conditional loss scheme. Specifically, the Flow Matching loss for the video modality ($\mathcal{L}_{\text{FM-video}}$) is only computed for samples originating from these two datasets when the diffusion timestep t exceeds an empirically determined threshold. We set this threshold to $\tau = 800$ (out of 1000 total timesteps). This strategy is predicated on the principle that at high noise levels (i.e., for $t > \tau$), the model learns to capture coarse, low-frequency features of the video, such as general motion and structure, which are less affected by the poor visual quality. By excluding the loss calculation at lower noise levels, we prevent the model from overfitting to the high-frequency visual artifacts and noise present in these datasets. The loss for video modality is:

$$\mathcal{L}_{\text{FM-video}} = \begin{cases} \mathcal{L}_{\text{FM}}(x_1, x_0, t) & \text{if } x_1 \in \Theta \text{ or } (x_1 \in \zeta \text{ and } t > 800) \\ 0 & \text{else} \end{cases}$$

where $x_0 \sim p_0$ is noise sample, $x_1 \sim p_1$ is data sample, ζ is data subset include vggSound and audioset, Θ is data subset exclude vggSound and audioset. The final training objective is a weighted sum of the flow matching and semantic alignment losses:

$$\mathcal{L} = \mathcal{L}_{\text{FM-video}} + \mathcal{L}_{\text{FM-mel}} + \lambda_{SSL} \cdot \mathcal{L}_{SSL}$$

where \mathcal{L}_{SSL} is a hyperparameter controlling the influence of the SSL guidance, empirically set to 1.0 according to Ace-step.

3.3 INDEPENDENT NOISE SAMPLING STRATEGY

Our empirical investigation reveals a critical sensitivity of multi-modal diffusion models to the pseudo-random number generation process. When a single, fixed random seed is used to initialize a training run, the noise tensors for the video (ϵ_v) and audio (ϵ_a) modalities are sampled sequentially

324 from the same deterministic PRNG sequence. Due to the deterministic nature of the underlying
 325 algorithm (Linear Congruential method), this sequential sampling introduces a spurious structural
 326 correlation between the two noise tensors, which can be expressed as $\epsilon_a = f(\epsilon_v)$. This violates the
 327 critical assumption that the noise vectors are statistically independent.

328 The model inadvertently learns this spurious correlation as a shortcut during training. Consequently,
 329 during inference, any alteration to the sampling of ϵ_v , such as a change in video resolution or duration,
 330 propagates through the PRNG’s state and alters the structure of the subsequently sampled ϵ_a . This
 331 mismatch with the learned correlation results in a significant degradation of the audio generation
 332 quality.

333 To address this, we propose an **Independent Noise Sampling Strategy**. This approach isolates
 334 the noise generation for each modality by employing separate and independently seeded PRNG
 335 instances. This method effectively breaks the deterministic correlation, ensuring the noise vectors
 336 are statistically independent. As a result, the model becomes robust to variations in inference-time
 337 conditions, mitigating the issue of performance degradation.

339 4 EXPERIMENTS

340 4.1 SETUP

343 **Implementation Details** The training is conducted with an effective batch size of 128 over 50k
 344 steps on a 7,600-hour audio-visual datasets built by our data curation pipeline (Appendix. B for more
 345 details), using the AdamW optimizer with a learning rate of $5e - 6$. We employ Fully Sharded Data
 346 Parallel (FSDP) for distributed training across multiple nodes, with a gradient accumulation step of 4.
 347

348 **Compared Methods** We conduct a comprehensive evaluation of our model by benchmarking it
 349 against a suite of state-of-the-art baselines across several distinct generation tasks, the details are in
 350 Appendix. D. It is important to note that our model is constructed by stitching the pre-trained WAN2.1
 351 (1.3B) and Step-Ace (3.5B) models. Consequently, the comparisons against the state-of-the-art
 352 baselines are intended to provide a qualitative reference and situate our work, rather than to make a
 353 direct claim of superior performance.

354 **Benchmark** To construct our evaluation set, we curated 600 image-text prompt pairs from a
 355 multitude of sources. These sources encompass frames extracted from YouTube videos, BiliBili
 356 videos, TikTok clips, movies, and anime; images generated by AI models (ByteDance, 2025; Wu
 357 et al., 2025); and a collection of images from public websites. More details are in Appendix. A.1

359 **Evaluation Protocol** We quantitatively evaluate our method against baselines on the Verse-Bench
 360 benchmark. The evaluation is structured across 6 distinct generation tasks, each with a tailored set of
 361 metrics. More details are in Appendix. E.1.

363 To provide a holistic, quantitative comparison of joint audio-video generation capabilities, we
 364 introduce a composite **Overall Score**. This score is formulated as a weighted average of four
 365 sub-scores, reflecting different aspects of model performance:

$$367 \quad \text{Overall Score} = 0.5 * S_{\text{joint}} + 0.2 * S_{\text{video}} + 0.2 * S_{\text{audio}} + 0.1 * S_{\text{other}}$$

369 Reflecting our emphasis on the core task, the *Joint Quality Score* (S_{joint}) constitutes 50% of the
 370 total weight. To strongly couple audio-video temporal alignment (AV-A) with audio-text semantic
 371 consistency (CS), we compute S_{joint} using the harmonic mean of their normalized values. This
 372 ensures that a high score is achieved only when both metrics are strong, heavily penalizing models
 373 that excel at synchronization but fail on content relevance. The remaining scores for video (S_{video}),
 374 audio (S_{audio}), and other modalities (S_{other}) are the arithmetic means of their respective metrics.

375 To ensure fair aggregation across metrics with different scales and trends, all individual metrics are
 376 first normalized to a unified range where higher is always better. For metrics with an upward trend (\uparrow),
 377 we use standard min-max scaling: $(\text{value} - \text{worst}) / (\text{best} - \text{worst})$. For metrics with a downward trend
 378 (\downarrow), we use an inverted formula: $(\text{worst} - \text{value}) / (\text{worst} - \text{best})$. More details are in Appendix. E.2.

378 Table 1: Quantitative results on Verse-Bench. Best results are in **bold**, second best are
 379 underlined.*When computing overall score for SVG, we set WER to 1.0 and LSE-C to 0.0.
 380

381	Methods	382 Video				383 Audio				384 TTS		385 Audio-Video		386 Overall Score ↑
		387 AS ↑	388 ID ↑	389 FD ↓	390 KL ↓	391 CS ↑	392 CE ↑	393 CU ↑	394 PC ↓	395 PQ ↑	396 WER ↓	397 LSE-C ↑	398 AV-A ↓	
383 Video 384 Methods	CogVideox1.5 SB	0.44	0.83	-	-	-	-	-	-	-	-	-	-	-
	Wan2.2-14B	0.50	<u>0.88</u>	-	-	-	-	-	-	-	-	-	-	-
	Kling2.1	0.41	0.85	-	-	-	-	-	-	-	-	-	-	-
	SeeDance1.0	0.47	0.86	-	-	-	-	-	-	-	-	-	-	-
386 Audio 387 Methods	Stable Audio	-	-	1.13	1.38	0.28	3.88	6.15	2.60	6.53	-	-	-	-
	AudioLdm2	-	-	1.21	2.30	0.24	3.98	<u>5.88</u>	3.43	6.04	-	-	-	-
388 TTS 389 Methods	Cosyvoice	-	-	-	-	-	-	-	-	-	0.17	-	-	-
	Cosyvoice2	-	-	-	-	-	-	-	-	-	<u>0.16</u>	-	-	-
	VibeVoice	-	-	-	-	-	-	-	-	-	0.15	-	-	-
390 A2V 391 Methods	Fantasy-Talking	0.42	0.87	-	-	-	-	-	-	-	-	<u>2.68</u>	-	-
	Wan-S2V	0.46	0.89	-	-	-	-	-	-	-	-	6.49	-	-
392 V2A 393 Method	HunyuanVideo-Foley	-	-	0.82	1.27	0.40	4.04	5.72	3.09	<u>6.27</u>	-	-	0.78	-
394 Joint 395 Methods	SVG	0.41	0.25	1.55	3.62	0.08	2.93	5.50	2.35	6.26	-	-	0.09	0.220*
	Ovi	0.52	0.89	-	-	0.09	4.89	6.04	2.20	6.23	0.28	4.85	0.51	0.408
	Ours	0.47	0.89	1.25	2.70	0.16	3.53	4.61	2.49	5.20	0.18	1.34	<u>0.23</u>	0.403

399 4.2 QUANTITATIVE EVALUATION

400 We compare Universe-1 against a range of state-of-the-art (SOTA) models specialized for specific
 401 tasks as shown in Tab. 1. As a unified joint generation model, a direct comparison of single-modality
 402 metrics against these "expert" models presents inherent complexities. Nevertheless, our model
 403 demonstrates robust capabilities across multiple dimensions.

404 In terms of video quality, Universe-1 achieves the highest score in identity preservation (ID: 0.89),
 405 showcasing its superior ability to maintain subject consistency throughout the generation process.
 406 For audio quality, while there is a gap compared to leading audio-only generation models, our model
 407 obtains a highly competitive score in pitch correlation (PC: 2.49).

408 The core strength of our model lies in synchronous audio-video generation. It is crucial to interpret
 409 the metrics for such joint generation tasks with caution. For instance, in the video-to-audio (V2A)
 410 setting, the AV-A metric for a model like Hunyuanvideo-Foley is calculated with a ground-truth video,
 411 whereas our model generates both modalities simultaneously. Therefore, AV-A must be considered
 412 in conjunction with the audio-text CLAP score (CS) for a holistic assessment. From this integrated
 413 perspective, our model (AV-A: 0.23, CS: 0.16) demonstrates a better overall audio-visual content
 414 consistency than SVG (AV-A: 0.09, CS: 0.08).

415 Similarly, for the lip-sync (LSE-C) metric, our model's score (1.34) is evaluated on fully generated
 416 audio and video, making it susceptible to the quality of both generated modalities. In contrast,
 417 audio-to-video (A2V) methods like Wan-S2V are evaluated using ground-truth audio, which naturally
 418 yields a higher score (6.49). Despite this evaluation disparity, Universe-1 achieves promising results
 419 as the first open-source joint generation framework of its kind, establishing a solid foundation for
 420 future research.

421 To encapsulate the model's holistic performance across these diverse and complex trade-offs, we
 422 designed a composite Overall Score detailed in the appendix. Ultimately, Universe-1 achieves
 423 a superior Overall Score of 0.403, substantially outperforming the SVG baseline (0.220). This
 424 result quantitatively validates the effectiveness of our approach and establishes Universe-1 as a
 425 state-of-the-art, well-balanced joint generation model.

426 4.3 USER STUDY

427 We conducted a user study, the details and results of which are presented in Appendix F.

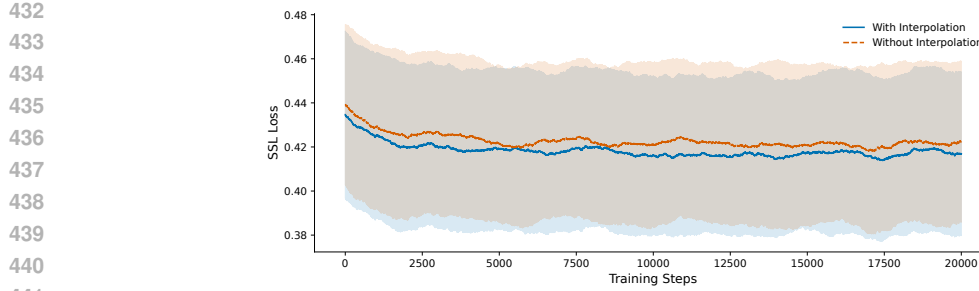


Figure 3: **Ablation study on Linearly Interpolating.** SSL Loss with(blue) and without(red) Linearly Interpolating.

Table 2: Ablation study on the effectiveness of our proposed components. The Overall Score is a composite metric detailed in the appendix. Removing either component degrades performance, validating their contribution.

Method	Video				Audio				TTS		Audio-Video		Overall Score ↑
	AS ↑	ID ↑	FD ↓	KL ↓	CS ↑	CE ↑	CU ↑	PC ↓	PQ ↑	WER ↓	LSE-C ↑	AV-A ↓	
w/o LQLS	0.44	0.78	1.26	2.84	0.15	3.38	4.35	2.58	4.97	0.16	1.35	0.28	0.378
w/o INSS	0.43	0.75	1.43	3.51	0.11	2.44	3.14	2.92	3.99	0.38	0.99	0.18	0.316
Ours	0.47	0.89	1.25	2.70	0.16	3.53	4.61	2.49	5.20	0.18	1.34	0.23	0.403

4.4 ABLATION STUDY

We performed an ablation study to investigate the contributions of our Low Quality data Loss Strategy(LQLS) and Independent Noise Sampling Strategy(INSS), as shown in Tab. 2. The findings indicate that LQLS provides improvement accross video quality and consistency ID, thus confirming its efficacy and positive impact on training. Furthermore, the results for INSS demonstrate a significant enhancement in audio generation quality, validating the effectiveness of this approach.

We also conducted an ablation study to validate the effectiveness of initializing parameters via linear interpolation within our layer interpolation technique. We provide a visual comparison of the semantic alignment loss, as shown in the Fig. 3. The results indicate that with interpolated initialization, the model exhibits a superior capacity for continued learning. Compared to randomly initializing the new layers, our approach aligns with the correct audio semantics much earlier in the training process.

5 LIMITATION AND FUTURE WORK

The work presented herein constitutes an initial exploration into unified audio-video generation. Our study was constrained by computational resources, necessitating that we conduct training exclusively on the Wan2.1-1.3B video model. The performance of our model is, therefore, inherently limited by the capacity of this base model. In the future, our research will focus on two key directions. First, we will scale up our experiments to larger video foundation models. Second, we will engage in more extensive and refined data curation efforts. The ultimate objective is to significantly advance the capabilities of open-source audio-video synthesis models, thereby bridging the performance gap to state-of-the-art proprietary models.

6 CONCLUSION

In this paper, we presented UniVerse-1, a novel framework for joint audio-video synthesis, achieved through the deep integration of a video foundation model and a music generation model using stitching of experts. Following fine-tuning on the dataset we curated, we also introduced Verse-Bench, a comprehensive benchmark to foster comparative research. To promote reproducibility and further innovation, our model and code have been made publicly available. Our experimental results validate

486 that this methodology offers a viable and efficient pathway for building sophisticated multimodal
 487 generative models by leveraging pre-existing unimodal foundations.
 488

489 **REFERENCES**
 490

491 Andreas Blattmann, Tim Dockhorn, Sumith Kulal, Daniel Mendelevitch, Maciej Kilian, Dominik
 492 Lorenz, Yam Levi, Zion English, Vikram Voleti, Adam Letts, et al. Stable video diffusion: Scaling
 493 latent video diffusion models to large datasets. *arXiv preprint arXiv:2311.15127*, 2023.

494 Marcely Zanon Boito, Vivek Iyer, Nikolaos Lagos, Laurent Besacier, and Ioan Calapodescu. mhubert-
 495 147: A compact multilingual hubert model. *arXiv preprint arXiv:2406.06371*, 2024.

496 ByteDance. Jimeng ai, 2025. URL <https://jimeng.jianying.com/>.

497 Honglie Chen, Weidi Xie, Andrea Vedaldi, and Andrew Zisserman. Vggsound: A large-scale audio-
 498 visual dataset. In *ICASSP 2020-2020 IEEE International Conference on Acoustics, Speech and
 499 Signal Processing (ICASSP)*, pp. 721–725. IEEE, 2020.

500 Junyu Chen, Han Cai, Junsong Chen, Enze Xie, Shang Yang, Haotian Tang, Muyang Li, Yao Lu, and
 501 Song Han. Deep compression autoencoder for efficient high-resolution diffusion models. *arXiv
 502 preprint arXiv:2410.10733*, 2024.

503 Yi Chen, Sen Liang, Zixiang Zhou, Ziyao Huang, Yifeng Ma, Junshu Tang, Qin Lin, Yuan Zhou,
 504 and Qinglin Lu. Hunyuuanvideo-avatar: High-fidelity audio-driven human animation for multiple
 505 characters. *arXiv preprint arXiv:2505.20156*, 2025.

506 Hyung Won Chung, Noah Constant, Xavier Garcia, Adam Roberts, Yi Tay, Sharan Narang, and
 507 Orhan Firat. Unimax: Fairer and more effective language sampling for large-scale multilingual
 508 pretraining. *arXiv preprint arXiv:2304.09151*, 2023.

509 Joon Son Chung and Andrew Zisserman. Out of time: automated lip sync in the wild. In *Asian
 510 conference on computer vision*, pp. 251–263. Springer, 2016.

511 Google DeepMind. Veo 2. <https://deepmind.google/technologies/veo/veo-2/>, 2024.12.

512 Google DeepMind. Veo 3. <https://deepmind.google/models/veo/>, 2025.5.

513 Jiankang Deng, Jia Guo, Evangelos Ververas, Irene Kotsia, and Stefanos Zafeiriou. Retinaface:
 514 Single-shot multi-level face localisation in the wild. In *Proceedings of the IEEE/CVF conference
 515 on computer vision and pattern recognition*, pp. 5203–5212, 2020.

516 discuss0434. aesthetic-predictor-v2-5, 2024. URL <https://github.com/discuss0434/aesthetic-predictor-v2-5/>.

517 Zhihao Du, Qian Chen, Shiliang Zhang, Kai Hu, Heng Lu, Yexin Yang, Hangrui Hu, Siqi Zheng,
 518 Yue Gu, Ziyang Ma, et al. Cosyvoice: A scalable multilingual zero-shot text-to-speech synthesizer
 519 based on supervised semantic tokens. *arXiv preprint arXiv:2407.05407*, 2024a.

520 Zhihao Du, Yuxuan Wang, Qian Chen, Xian Shi, Xiang Lv, Tianyu Zhao, Zhifu Gao, Yexin Yang,
 521 Changfeng Gao, Hui Wang, et al. Cosyvoice 2: Scalable streaming speech synthesis with large
 522 language models. *arXiv preprint arXiv:2412.10117*, 2024b.

523 Alex Ergasti, Giuseppe Gabriele Tarollo, Filippo Botti, Tomaso Fontanini, Claudio Ferrari, Massimo
 524 Bertozzi, and Andrea Prati. R-flav: Rolling flow matching for infinite audio video generation.
 525 *arXiv preprint arXiv:2503.08307*, 2025.

526 Zach Evans, Julian D Parker, CJ Carr, Zack Zukowski, Josiah Taylor, and Jordi Pons. Stable audio
 527 open. In *ICASSP 2025-2025 IEEE International Conference on Acoustics, Speech and Signal
 528 Processing (ICASSP)*, pp. 1–5. IEEE, 2025.

529 Seth Forsgren and Hayk Martiros. Riffusion: Stable diffusion for real-time music generation.
 530 <https://github.com/riffusion/riffusion>, 2022.

540 Xin Gao, Li Hu, Siqi Hu, Mingyang Huang, Chaonan Ji, Dechao Meng, Jinwei Qi, Penchong Qiao,
 541 Zhen Shen, Yafei Song, et al. Wan-s2v: Audio-driven cinematic video generation. *arXiv preprint*
 542 *arXiv:2508.18621*, 2025a.

543

544 Yu Gao, Haoyuan Guo, Tuyen Hoang, Weilin Huang, Lu Jiang, Fangyuan Kong, Huixia Li, Jiashi Li,
 545 Liang Li, Xiaojie Li, et al. Seedance 1.0: Exploring the boundaries of video generation models.
 546 *arXiv preprint arXiv:2506.09113*, 2025b.

547

548 Jort F Gemmeke, Daniel PW Ellis, Dylan Freedman, Aren Jansen, Wade Lawrence, R Channing
 549 Moore, Manoj Plakal, and Marvin Ritter. Audio set: An ontology and human-labeled dataset for
 550 audio events. In *2017 IEEE international conference on acoustics, speech and signal processing*
 (ICASSP), pp. 776–780. IEEE, 2017.

551

552 Junmin Gong, Sean Zhao, Sen Wang, Shengyuan Xu, and Joe Guo. Ace-step: A step towards music
 553 generation foundation model. *arXiv preprint arXiv:2506.00045*, 2025.

554

555 Yuwei Guo, Ceyuan Yang, Anyi Rao, Zhengyang Liang, Yaohui Wang, Yu Qiao, Maneesh Agrawala,
 556 Dahua Lin, and Bo Dai. Animatediff: Animate your personalized text-to-image diffusion models
 557 without specific tuning. *arXiv preprint arXiv:2307.04725*, 2023.

558

559 R Hamming. Mathematical methods in large-scale computing units. *Math Rev*, 13(1):495, 1952.

560

561 Akio Hayakawa, Masato Ishii, Takashi Shibuya, and Yuki Mitsufuji. Mmdisco: Multi-modal
 562 discriminator-guided cooperative diffusion for joint audio and video generation. *arXiv preprint*
 563 *arXiv:2405.17842*, 2024.

564

565 Jonathan Ho, Tim Salimans, Alexey Gritsenko, William Chan, Mohammad Norouzi, and David J
 566 Fleet. Video diffusion models. *Advances in neural information processing systems*, 35:8633–8646,
 567 2022.

568

569 Vladimir Iashin, Weidi Xie, Esa Rahtu, and Andrew Zisserman. Synchformer: Efficient synchronization
 570 from sparse cues. In *ICASSP 2024-2024 IEEE International Conference on Acoustics, Speech
 571 and Signal Processing (ICASSP)*, pp. 5325–5329. IEEE, 2024.

572

573 Masato Ishii, Akio Hayakawa, Takashi Shibuya, and Yuki Mitsufuji. A simple but strong baseline
 574 for sounding video generation: Effective adaptation of audio and video diffusion models for joint
 575 generation. *arXiv preprint arXiv:2409.17550*, 2024.

576

577 Junjie Ke, Qifei Wang, Yilin Wang, Peyman Milanfar, and Feng Yang. Musiq: Multi-scale image
 578 quality transformer. In *Proceedings of the IEEE/CVF international conference on computer vision*,
 579 pp. 5148–5157, 2021.

580

581 Qiuqiang Kong, Yin Cao, Turab Iqbal, Yuxuan Wang, Wenwu Wang, and Mark D Plumbley. Panns:
 582 Large-scale pretrained audio neural networks for audio pattern recognition. *IEEE/ACM Transactions
 583 on Audio, Speech, and Language Processing*, 28:2880–2894, 2020.

584

585 Weijie Kong, Qi Tian, Zijian Zhang, Rox Min, Zuozhuo Dai, Jin Zhou, Jiangfeng Xiong, Xin Li,
 586 Bo Wu, Jianwei Zhang, et al. Hunyuandvideo: A systematic framework for large video generative
 587 models. *arXiv preprint arXiv:2412.03603*, 2024.

588

589 Khaled Koutini, Jan Schlüter, Hamid Eghbal-Zadeh, and Gerhard Widmer. Efficient training of audio
 590 transformers with patchout. *arXiv preprint arXiv:2110.05069*, 2021.

591

592 Kuaishou. Kling ai. <https://klingai.kuaishou.com/>, 2024.06.

593

594 Seung Hyun Lee, Gyeongrok Oh, Wonmin Byeon, Chanyoung Kim, Won Jeong Ryoo, Sang Ho
 595 Yoon, Hyunjung Cho, Jihyun Bae, Jinkyu Kim, and Sangpil Kim. Sound-guided semantic video
 596 generation. In *European Conference on Computer Vision*, pp. 34–50. Springer, 2022.

597

598 Rui long Li, Shan Yang, David A Ross, and Angjoo Kanazawa. Ai choreographer: Music conditioned
 599 3d dance generation with aist++. In *Proceedings of the IEEE/CVF international conference on
 600 computer vision*, pp. 13401–13412, 2021.

594 Yizhi Li, Ruibin Yuan, Ge Zhang, Yinghao Ma, Xingran Chen, Hanzhi Yin, Chenghao Xiao,
 595 Chenghua Lin, Anton Ragni, Emmanouil Benetos, et al. Mert: Acoustic music understanding
 596 model with large-scale self-supervised training. *arXiv preprint arXiv:2306.00107*, 2023.

597

598 Shijia Liao, Yuxuan Wang, Tianyu Li, Yifan Cheng, Ruoyi Zhang, Rongzhi Zhou, and Yijin Xing.
 599 Fish-speech: Leveraging large language models for advanced multilingual text-to-speech synthesis.
 600 *arXiv preprint arXiv:2411.01156*, 2024.

601

602 Gaojie Lin, Jianwen Jiang, Jiaqi Yang, Zerong Zheng, and Chao Liang. Omnihuman-1: Rethinking the
 603 scaling-up of one-stage conditioned human animation models. *arXiv preprint arXiv:2502.01061*,
 604 2025.

605 Yaron Lipman, Ricky TQ Chen, Heli Ben-Hamu, Maximilian Nickel, and Matt Le. Flow matching
 606 for generative modeling. *arXiv preprint arXiv:2210.02747*, 2022.

607

608 Haohe Liu, Zehua Chen, Yi Yuan, Xinhao Mei, Xubo Liu, Danilo Mandic, Wenwu Wang, and Mark D
 609 Plumbley. AudioLDM: Text-to-audio generation with latent diffusion models. *Proceedings of the
 610 International Conference on Machine Learning*, pp. 21450–21474, 2023.

611

612 Haohe Liu, Gael Le Lan, Xinhao Mei, Zhaoheng Ni, Anurag Kumar, Varun Nagaraja, Wenwu Wang,
 613 Mark D Plumbley, Yangyang Shi, and Vikas Chandra. Syncflow: Toward temporally aligned joint
 614 audio-video generation from text. *arXiv preprint arXiv:2412.15220*, 2024a.

615

616 Haohe Liu, Yi Yuan, Xubo Liu, Xinhao Mei, Qiuqiang Kong, Qiao Tian, Yuping Wang, Wenwu
 617 Wang, Yuxuan Wang, and Mark D. Plumbley. Audioldm 2: Learning holistic audio generation with
 618 self-supervised pretraining. *IEEE/ACM Transactions on Audio, Speech, and Language Processing*,
 32:2871–2883, 2024b. doi: 10.1109/TASLP.2024.3399607.

619

620 Yuxuan Luo, Zhengkun Rong, Lizhen Wang, Longhao Zhang, Tianshu Hu, and Yongming Zhu.
 621 Dreamactor-m1: Holistic, expressive and robust human image animation with hybrid guidance.
 622 *arXiv preprint arXiv:2504.01724*, 2025.

623

624 Guoqing Ma, Haoyang Huang, Kun Yan, Liangyu Chen, Nan Duan, Shengming Yin, Changyi Wan,
 625 Ranchen Ming, Xiaoniu Song, Xing Chen, et al. Step-video-t2v technical report: The practice,
 challenges, and future of video foundation model. *arXiv preprint arXiv:2502.10248*, 2025.

626

627 Ziqian Ning, Huakang Chen, Yuepeng Jiang, Chunbo Hao, Guobin Ma, Shuai Wang, Jixun Yao,
 628 and Lei Xie. Diffrrhythm: Blazingly fast and embarrassingly simple end-to-end full-length song
 629 generation with latent diffusion. *arXiv preprint arXiv:2503.01183*, 2025.

630

631 OpenAI. Video generation models as world simulators, 2024. URL <https://openai.com/index/video-generation-models-as-world-simulators/>.

632

633 William Peebles and Saining Xie. Scalable diffusion models with transformers. In *Proceedings of
 634 the IEEE/CVF international conference on computer vision*, pp. 4195–4205, 2023.

635

636 Zhiliang Peng, Jianwei Yu, Wenhui Wang, Yaoyao Chang, Yutao Sun, Li Dong, Yi Zhu, Weijiang Xu,
 637 Hangbo Bao, Zehua Wang, et al. Vibevoice technical report. *arXiv preprint arXiv:2508.19205*,
 2025.

638

639 Adam Polyak, Amit Zohar, Andrew Brown, Andros Tjandra, Animesh Sinha, Ann Lee, Apoorv Vyas,
 640 Bowen Shi, Chih-Yao Ma, Ching-Yao Chuang, et al. Movie gen: A cast of media foundation
 641 models. *arXiv preprint arXiv:2410.13720*, 2024.

642

643 Alec Radford, Jong Wook Kim, Tao Xu, Greg Brockman, Christine McLeavey, and Ilya Sutskever.
 644 Robust speech recognition via large-scale weak supervision. In *International conference on
 645 machine learning*, pp. 28492–28518. PMLR, 2023.

646

647 Robin Rombach, Andreas Blattmann, Dominik Lorenz, Patrick Esser, and Björn Ommer. High-
 resolution image synthesis with latent diffusion models. In *Proceedings of the IEEE/CVF confer-
 ence on computer vision and pattern recognition*, pp. 10684–10695, 2022.

648 Ludan Ruan, Yiyang Ma, Huan Yang, Huiguo He, Bei Liu, Jianlong Fu, Nicholas Jing Yuan, Qin
 649 Jin, and Baining Guo. Mm-diffusion: Learning multi-modal diffusion models for joint audio and
 650 video generation. In *Proceedings of the IEEE/CVF Conference on Computer Vision and Pattern*
 651 *Recognition*, pp. 10219–10228, 2023.

652 Sizhe Shan, Qiulin Li, Yutao Cui, Miles Yang, Yuehai Wang, Qun Yang, Jin Zhou, and Zhao Zhong.
 653 Hunyuandvideo-foley: Multimodal diffusion with representation alignment for high-fidelity foley
 654 audio generation. *arXiv preprint arXiv:2508.16930*, 2025.

655 Oriane Siméoni, Huy V Vo, Maximilian Seitzer, Federico Baldassarre, Maxime Oquab, Cijo Jose,
 656 Vasil Khalidov, Marc Szafraniec, Seungeun Yi, Michaël Ramamonjisoa, et al. Dinov3. *arXiv*
 657 *preprint arXiv:2508.10104*, 2025.

658 Yang Song and Stefano Ermon. Improved techniques for training score-based generative models.
 659 *Advances in neural information processing systems*, 33:12438–12448, 2020.

660 Yang Song, Jascha Sohl-Dickstein, Diederik P Kingma, Abhishek Kumar, Stefano Ermon, and Ben
 661 Poole. Score-based generative modeling through stochastic differential equations. *arXiv preprint*
 662 *arXiv:2011.13456*, 2020.

663 Shuai Tan, Biao Gong, Xiang Wang, Shiwei Zhang, Dandan Zheng, Ruobing Zheng, Kecheng Zheng,
 664 Jingdong Chen, and Ming Yang. Animate-x: Universal character image animation with enhanced
 665 motion representation. *arXiv preprint arXiv:2410.10306*, 2024.

666 Andros Tjandra, Yi-Chiao Wu, Baishan Guo, John Hoffman, Brian Ellis, Apoorv Vyas, Bowen Shi,
 667 Sanyuan Chen, Matt Le, Nick Zacharov, et al. Meta audiobox aesthetics: Unified automatic quality
 668 assessment for speech, music, and sound. *arXiv preprint arXiv:2502.05139*, 2025.

669 Team Wan, Ang Wang, Baole Ai, Bin Wen, Chaojie Mao, Chen-Wei Xie, Di Chen, Feiwu Yu,
 670 Haiming Zhao, Jianxiao Yang, et al. Wan: Open and advanced large-scale video generative models.
 671 *arXiv preprint arXiv:2503.20314*, 2025.

672 Duomin Wang, Yu Deng, Zixin Yin, Heung-Yeung Shum, and Baoyuan Wang. Progressive disentan-
 673 gled representation learning for fine-grained controllable talking head synthesis. In *Proceedings of*
 674 *the IEEE/CVF Conference on Computer Vision and Pattern Recognition*, pp. 17979–17989, 2023.

675 Mengchao Wang, Qiang Wang, Fan Jiang, Yaqi Fan, Yunpeng Zhang, Yonggang Qi, Kun Zhao, and
 676 Mu Xu. Fantasytalking: Realistic talking portrait generation via coherent motion synthesis. *arXiv*
 677 *preprint arXiv:2504.04842*, 2025.

678 Chenfei Wu, Jiahao Li, Jingren Zhou, Junyang Lin, Kaiyuan Gao, Kun Yan, Sheng-ming Yin, Shuai
 679 Bai, Xiao Xu, Yilei Chen, et al. Qwen-image technical report. *arXiv preprint arXiv:2508.02324*,
 680 2025.

681 Haoning Wu, Erli Zhang, Liang Liao, Chaofeng Chen, Jingwen Hou, Annan Wang, Wenxiu Sun,
 682 Qiong Yan, and Weisi Lin. Exploring video quality assessment on user generated contents from
 683 aesthetic and technical perspectives. In *Proceedings of the IEEE/CVF International Conference on*
 684 *Computer Vision*, pp. 20144–20154, 2023a.

685 Yusong Wu, Ke Chen, Tianyu Zhang, Yuchen Hui, Taylor Berg-Kirkpatrick, and Shlomo Dubnov.
 686 Large-scale contrastive language-audio pretraining with feature fusion and keyword-to-caption
 687 augmentation. In *ICASSP 2023-2023 IEEE International Conference on Acoustics, Speech and*
 688 *Signal Processing (ICASSP)*, pp. 1–5. IEEE, 2023b.

689 Jin Xu, Zhifang Guo, Jinzheng He, Hangrui Hu, Ting He, Shuai Bai, Keqin Chen, Jialin Wang, Yang
 690 Fan, Kai Dang, et al. Qwen2. 5-omni technical report. *arXiv preprint arXiv:2503.20215*, 2025.

691 Sidi Yang, Tianhe Wu, Shuwei Shi, Shanshan Lao, Yuan Gong, Mingdeng Cao, Jiahao Wang, and
 692 Yujiu Yang. Maniqa: Multi-dimension attention network for no-reference image quality assessment.
 693 In *Proceedings of the IEEE/CVF conference on computer vision and pattern recognition*, pp. 1191–
 694 1200, 2022.

702 Zhuoyi Yang, Jiayan Teng, Wendi Zheng, Ming Ding, Shiyu Huang, Jiazheng Xu, Yuanming Yang,
703 Wenyi Hong, Xiaohan Zhang, Guanyu Feng, et al. Cogvideox: Text-to-video diffusion models
704 with an expert transformer. *arXiv preprint arXiv:2408.06072*, 2024.

705
706 Zhentao Yu, Zixin Yin, Deyu Zhou, Duomin Wang, Finn Wong, and Baoyuan Wang. Talking head
707 generation with probabilistic audio-to-visual diffusion priors. In *Proceedings of the IEEE/CVF*
708 *International Conference on Computer Vision*, pp. 7645–7655, 2023.

709 Lei Zhao, Linfeng Feng, Dongxu Ge, Rujin Chen, Fangqiu Yi, Chi Zhang, Xiao-Lei Zhang, and
710 Xuelong Li. Uniform: A unified multi-task diffusion transformer for audio-video generation. *arXiv*
711 *preprint arXiv:2502.03897*, 2025.

712

713

714

715

716

717

718

719

720

721

722

723

724

725

726

727

728

729

730

731

732

733

734

735

736

737

738

739

740

741

742

743

744

745

746

747

748

749

750

751

752

753

754

755

APPENDIX

A MORE DETAILS ABOUT VERSE-BENCH

A.1 DETAILED DESCRIPTION

Our dataset comprises three subsets.

- Set1-I contains image-text pairs (including AI-generated, web-crawled, and media screenshots), for which video/audio captions and speech content were produced using LLMs (Xu et al., 2025) and manual annotation, comprising a total of 205 samples. Statistical results in 6.
- Set2-V consists of video clips from YouTube and Bilibili, which were annotated with LLM-generated (Xu et al., 2025) captions and Whisper-based ASR (Radford et al., 2023) transcripts, followed by human verification, comprising a total of 295 samples. Statistical results in 7.
- Set3-Ted (the Verse-Ted subset) includes TED Talks from September 2025, processed with the same annotation pipeline as Set2, comprising a total of 100 samples.

Our collected test data is highly diverse, encompassing a wide spectrum of audio categories: human speech; animal vocalizations (e.g., bird chirping, cat meowing); instrumental music (e.g., piano, guitar); natural sounds (e.g., thunder, rain); human-object interactions (e.g., keyboard typing, cooking, chopping vegetables); object-object interactions (e.g., glass shattering, marbles dropping); mechanical sounds (e.g., trains, airplanes), and so on. The complete statistical results of set1 and set2 are shown in 5.

A.2 STATISTICAL RESULTS

This section provides the detailed category catalog for Verse-Bench, along with a high-resolution pie chart illustrating its statistical distribution in Fig. 5 6 7.

Category list is in Tab. 3, 4, 5.

B DATA CURATION

We curated a large-scale, high-quality dataset from a diverse range of sources to train our model. The primary component was sourced from YouTube, encompassing content such as music variety shows, classical music performances, cooking tutorials, public speeches, interviews, vlogs, and demonstrations of tool usage. This was supplemented with cinematic movie clips and high-quality stock footage from Pexels. To further bolster the audio modality, we also incorporated the widely-used VGGSound and AudioSet datasets.

For our self-collected data (YouTube, Pexels, and movie clips), we implemented a rigorous multi-stage filtering pipeline to ensure data quality and relevance:

- **Audio-Visual Pre-screening** Videos lacking an audio track were immediately discarded.
- **Quality Control** We filtered out content based on technical specifications: resolution below 1080p, a bitrate-to-resolution ratio under 600, and a DOVER (Wu et al., 2023a) aesthetic quality score below 0.6.
- **Temporal Coherence** PySceneDetect¹ was applied to segment videos, and any resulting clip shorter than 5 seconds was removed to ensure meaningful duration.
- **Audio Activity Detection** To eliminate silent segments, we analyzed each audio track for metrics such as volume, energy, and zero-crossing rate.
- **Speech Content Verification** Whisper (Radford et al., 2023) was used to detect the presence of human speech. Clips without speech were retained as general audio-visual data. If speech was present, it proceeded to the next step.

¹<https://github.com/Breakthrough/PySceneDetect>

810 • **Human Face Detection** For clips identified as containing speech, a second verification step was
 811 performed: we detected for the presence of a human face (Deng et al., 2020). If no face was found,
 812 the clip was discarded. If a face was present, we employed SyncNet (Chung & Zisserman, 2016)
 813 to verify the audio-visual correspondence (lip-sync). Only clips with a SyncNet confidence score
 814 above a threshold of 2.0 were retained and explicitly labeled as containing speech content.
 815

816 For the VGGSound and AudioSet data, a simplified process was used where we either performed
 817 scene detection or segmented clips based on their existing timestamps, retaining only those longer
 818 than 5 seconds.

819 Following this comprehensive curation process, our final dataset comprises 7,685 hours of data. This
 820 is categorized into three subsets: 1,187 hours of verified speech-centric content, 3,074 hours of
 821 general-purpose audio-video data, and 3,422 hours from VGGSound and AudioSet primarily used
 822 for bolstering audio-specific training.

823 C ONLINE DATA ANNOTATION

827 Conventional offline annotation methods, where captions are pre-generated for entire videos, present a
 828 significant challenge for training generative models. During training, fixed-length clips are randomly
 829 sampled from these videos, often creating a temporal and semantic misalignment between the sampled
 830 clip and the global, pre-existing caption. This issue is particularly acute in the context of joint audio-
 831 video generation, where the temporal synchronization between an acoustic event and its description
 832 is critical. Even minor temporal shifts can render an audio annotation invalid.

833 To overcome these limitations, we propose and implement an Online Data Annotation Pipeline. This
 834 pipeline operates as a dedicated server process that runs concurrently with training. It dynamically
 835 fetches raw video, processes clips in real-time to generate precisely aligned data-annotation pairs,
 836 and populates a shared buffer. The main training process then acts as a consumer, fetching these
 837 ready-to-use data tuples, ensuring that every training instance is perfectly synchronized.

838 The online processing for each data tuple involves the following steps:

840 • **Temporal Sampling** A fixed-length segment (e.g., 5 seconds) is randomly extracted from a source
 841 video, yielding corresponding video and audio streams.

843 • **Multi-modal Annotation** The extracted audio-video clip is immediately passed to our annotation
 844 module for captioning.

845 • **Text and Video Encoding** The generated text prompts (for video, audio, and speech) are encoded.
 846 Concurrently, the video clip is encoded into a spatio-temporal latent representation using the 3D
 847 VAE.

849 • **Audio Encoding** The audio stream is converted to a mel spectrogram and subsequently encoded
 850 into a latent representation by the Music-DCAE (Chen et al., 2024).

852 The core of our pipeline is the multi-modal annotation step (Step 2), which proceeds as follows:

854 • **Speech Transcription** Whisper (Radford et al., 2023) is employed to perform Automatic Speech
 855 Recognition (ASR) on the sampled audio, yielding the raw speech content.

856 • **Structured Multimodal Captioning** We construct a structured prompt that incorporates the
 857 transcribed speech. This prompt, along with the audio and video streams of the clip, is fed into
 858 the QWen2.5-Omni (Xu et al., 2025) multimodal model. QWen2.5-Omni is specifically instructed
 859 to output three distinct, aligned annotations for the clip: the verified speech content, a descriptive
 860 video caption, and a caption for the ambient audio.

862 This online, just-in-time process guarantees that every training instance consists of video and audio
 863 latents that are perfectly synchronized in time and semantically consistent with their corresponding
 864 textual annotations, thereby eliminating the data misalignment problem inherent in offline methods.

864 **D DETAILS ON COMPARED METHODS**
865866 We conduct a comprehensive evaluation of our model by benchmarking it against a suite of state-of-
867 the-art baselines across several distinct generation tasks:
868869

- 870 • Video Generation: We compare our model against leading text-to-video systems, including Wan2.2
871 (14B) (Wan et al., 2025), HunyuanVideo (Kong et al., 2024), CogVideoX-1.5, (5B) (Yang et al.,
872 2024), Kling 2.1 (Kuaishou, 2024.06), and SeeDance 1.0 (Gao et al., 2025b).
- 873 • Audio Generation: For the audio modality, we benchmark against established text-to-audio models
874 such as Stable Audio Open (Evans et al., 2025) and AudioLDM2 (Liu et al., 2024b).
- 875 • Text-to-Speech (TTS): As a supplementary evaluation of vocal synthesis, we compare our
876 model’s performance against specialized TTS models, including CosyVoice (Du et al., 2024a),
877 CosyVoice2 (Du et al., 2024b), and VibeVoice (Peng et al., 2025).
- 878 • Audio-to-Video methods: We also compare our model with talking-based audio to video methods
879 such as FantasyTalking (Wang et al., 2025) and Wan-S2V (Gao et al., 2025a).
- 880 • Video-to-Audio methods: As a closely related task to joint audio-visual generation, we also
881 benchmarked our model on the video-to-audio (V2A) task, drawing comparisons with state-of-the-
882 art methods such as HunyuanVideo-Foley (Shan et al., 2025).
- 883 • Joint Audio-Video Generation: For our core task of synchronous audio-visual synthesis, we
884 compare our method against existing prompt-based joint generation models: SVG (Ishii et al.,
885 2024). Since methods such as MM-Diffusion (Ruan et al., 2023) and R-FLAV (Ergasti et al., 2025)
886 are class-conditional generative models, a direct comparison with our approach is not applicable,
887 we only compare with SVG here.

888889 **E DETAILS ON EVALUATION PROTOCOL**
890891 **E.1 TASKS AND METRICS**892 The compared task and corresponding metrics are:
893894

- 895 • Video Generation: Performance is assessed on three criteria:
 - 896 – Aesthetic Score (AS): This is a composite score averaging three components: fidelity, measured
897 by MANIQA (Yang et al., 2022) to penalize blur and artifacts, and aesthetic quality, evaluated
898 by both aesthetic-predictor-v2-5 (discus0434, 2024) and Musiq (Ke et al., 2021).
 - 899 – ID Consistency (ID): To measure identity preservation, we compute the mean DI-
900 NOV3 (Siméoni et al., 2025) feature similarity between the reference image and each generated
901 frame.
- 902 • Audio Generation: We evaluate audio quality from three perspectives:
 - 903 – Distributional Similarity: We measure the Fréchet Distance (FD) and Kullback-Leibler (KL)
904 divergence between the generated and real data distributions, using features extracted from
905 PANNs (Kong et al., 2020) and PaSST (Koutini et al., 2021).
 - 906 – Semantic Consistency: The alignment between the audio and the input text is measured by the
907 LAION-CLAP (Wu et al., 2023b) score.
 - 908 – Quality and Diversity: We report the Inception Score (IS) calculated with a PANNs classifier.
909 Additionally, we use AudioBox-Aesthetics (Tjandra et al., 2025) to assess Production Quality
910 (PQ), Production Complexity (PC), Content Enjoyment (CE), and Content Usefulness (CU).
- 911 • Text-to-Speech (TTS): We evaluate synthesis accuracy using the Word Error Rate (WER), which
912 is derived by transcribing the generated audio with the Whisper-large-v3 model (Radford et al.,
913 2023).
- 914 • Audio-to-Video: We evaluate this task using the same criteria as the video generation task, ad-
915 ditionally providing a SyncNet (Chung & Zisserman, 2016) confidence score to assess lip-sync
916 accuracy.
- 917 • Video-to-Audio: This task use all metrics from audio generation tasks. Furthermore, we introduce
918 the Audio-Video Alignment (AV-A) metric to specifically quantify the temporal synchronization

918 between the generated audio and video streams, which is computed via Synchformer (Iashin et al.,
 919 2024).

920 • Joint Audio-Video Generation: For this task, we use all relevant metrics from the individual tasks
 921 above.

923 The evaluation of our models and their components is conducted across the three test sets as follows:

925 • The video generation models and SVG are evaluated on Set 1 and Set 2.
 926 • For the audio generation model is evaluated on Set1 and Set2.
 927 • The Text-to-Speech (TTS) model is primarily evaluated on Set 3.
 928 • The Audio-to-Video (A2V) model is evaluated exclusively on Set 3, while the Video-to-Audio
 929 (V2A) model is evaluated exclusively on Set 2.
 930 • Finally, our complete Universe-1 model is benchmarked against all three test sets.

932 For audio generation, we evaluate the metrics CE, CU, PC, and PQ on Set 1. On Set 2, the evaluation
 933 is expanded to include FD, KL, and CS in addition to the aforementioned metrics. Furthermore,
 934 LSE-C is evaluated exclusively on Set 3, while the AV-A metric is also applied to Set 1 when
 935 evaluating UniVerse-1 and SVG.

936 E.2 DETAILS ABOUT OVERALL SCORE

938 To provide a comprehensive and principled evaluation of model performance across multiple modalities,
 939 we designed a composite Overall Score. The primary motivation behind this metric is to create a
 940 single, holistic figure of merit that encapsulates the complex trade-offs inherent in joint audio-video
 941 generation, while placing a strong emphasis on the model’s core capabilities. The score is formulated
 942 as a weighted average of four distinct sub-scores:

$$943 \text{Overall}_{\text{Score}} = 0.5 * S_{\text{joint}} + 0.2 * S_{\text{video}} + 0.2 * S_{\text{audio}} + 0.1 * S_{\text{other}}$$

945 The components are defined as follows:

946 • Joint Quality Score (S_{joint}): This is the most critical component, receiving a 50% weight to reflect
 947 the primary focus of our work. Its purpose is to measure the quality of synchronous audio-video
 948 generation. A key insight is that temporal alignment (measured by AV-A) is only meaningful
 949 if the generated audio content is semantically relevant to the text prompt (measured by CS). To
 950 strongly couple these two aspects, we employ the harmonic mean of their normalized values. The
 951 harmonic mean is highly sensitive to lower values, ensuring a high score is achieved only when
 952 both alignment and content relevance are strong. A model with perfect alignment but irrelevant
 953 content, or vice-versa, will be heavily penalized.

954 • Video and Audio Quality Scores (S_{video} , S_{audio}): These sub-scores, each weighted at 20%, provide
 955 a balanced view of the model’s capabilities in generating high-quality content for each individual
 956 modality. They are calculated as the arithmetic mean of all normalized metrics within their
 957 respective categories.

958 • Other Modalities Score (S_{other}): This component, with a 10% weight, accounts for secondary
 959 capabilities such as Text-to-Speech (WER) and audio-driven lip-sync (LSE-C), ensuring the
 960 model’s versatility is also recognized.

961 **Metric Normalization** To ensure fair aggregation of metrics with different scales and trends (i.e.,
 962 some are better when higher, others when lower), all individual metrics are first normalized to a
 963 unified [0, 1] scale, where a higher score is always better. We use a robust normalization scheme
 964 based on fixed theoretical or empirical bounds, rather than the min-max values within our specific
 965 results table, to ensure the stability and generalizability of the score.

967 For upward-trending metrics (\uparrow), such as AS or CE, we use the formula:

$$968 \text{Normalized}_{\text{Score}} = (\text{value} - \text{worst}_{\text{bound}}) / (\text{best}_{\text{bound}} - \text{worst}_{\text{bound}})$$

970 For downward-trending metrics (\downarrow), such as FD or AV-A, we use an inverted formula to reverse the
 971 trend:

$$972 \text{Normalized}_{\text{Score}} = (\text{worst}_{\text{bound}} - \text{value}) / (\text{worst}_{\text{bound}} - \text{best}_{\text{bound}})$$

972 For metrics with a natural scale, such as the [1, 10] range for CE, CU, PQ, and PC, we use the
 973 scale’s limits as the best bound and worst bound. For unbounded metrics like FD and KL, we set
 974 a conservative empirical upper bound as the worst bound (e.g., 3.0 and 4.0, respectively) and their
 975 theoretical optimum of 0 as the best bound.
 976

977 **Handling of Missing Data** For models with missing metrics, such as the SVG baseline which
 978 lacks scores for WER and LSE-C, we performed imputation by assigning the worst possible values
 979 (e.g., WER=1.0, LSE-C=0.0). This conservative approach results in a normalized score of 0 for these
 980 imputed metrics, allowing for a direct and fair comparison without artificially inflating the baseline’s
 981 performance.

982 This carefully designed Overall Score provides a robust, interpretable, and single-figure metric that
 983 accurately reflects the strengths of a well-balanced, joint audio-video generation model.
 984

985 F USER STUDY

986 To provide a comprehensive qualitative assessment of our model’s capabilities, we conducted a user
 987 study comparing our method against state-of-the-art specialized models across six distinct generation
 988 tasks. The results, presented as user preference percentages in Fig. 4, are detailed below.
 989

990 F.1 DETAILS

991 Our user study was conducted with 17 participants, who were asked to independently evaluate the
 992 results from various methods across different tasks. For each task dimension, 10 comparison sets
 993 were provided. Following a standardized evaluation protocol, participants were instructed to rank
 994 the outputs of the different methods without allowing for ties. After collecting the rankings, we
 995 calculated the mean rank for each method to quantify the collective user preference. These mean
 996 ranks were subsequently normalized into percentages for final presentation.
 997

998 F.2 RESULTS

1000 **Key Findings** Our model, demonstrates a powerful and well-balanced performance profile as a
 1001 unified audio-video framework. Our model not only establishes a dominant lead in the core joint
 1002 generation task but also achieves SOTA or highly competitive results in complex directional tasks like
 1003 Text-to-Speech (TTS) and Audio-to-Video (A2V). The study validates that our *Stitching of Experts*
 1004 approach creates a versatile model that excels where multi-modal coherence is paramount.
 1005

1006 Task-Specific Analysis

- 1007 • **(a) Video-Only and (c) Audio-Only Generation:** In unimodal tasks, our model is predictably
 1008 surpassed by larger expert models. This is a direct reflection of using a more modest video
 1009 foundation, the Wan2.1 1.3B model, within a unified architecture, which naturally has a lower
 1010 intrinsic capability than the specialized SOTA systems.
- 1011 • **(b) Video-to-Audio (V2A) Generation:** The expert model, HunyuanVideo-Foley, achieves a
 1012 higher user preference in this specialized directional task.
- 1013 • **(e) Text-to-Speech (TTS) Generation:** Our model demonstrates a significant strength in text-to-
 1014 speech synthesis. In the Text Alignment metric, it outperforms both CosyVoice and CosyVoice2,
 1015 proving its ability to generate high-quality, semantically aligned audio from text is highly competi-
 1016 tive with SOTA TTS models.
- 1017 • **(f) Audio-to-Video (A2V) Generation:** The A2V results reveal a key advantage of our approach.
 1018 While a specialized model leads in Lip Sync, our model overwhelmingly outperforms all baselines
 1019 in Reference Consistency. This is a critical finding, indicating our model’s superior capability in
 1020 maintaining the subject’s identity and scene integrity, a vital component for realistic and coherent
 1021 video synthesis that specialized models often overlook.
- 1022 • **(d) Joint Audio-Video Generation:** This task provides the most holistic evaluation and represents
 1023 the core strength of our work. Our model demonstrates a dominant, landslide victory over the SVG
 1024 baseline across all five metrics. This substantial margin unequivocally establishes the superiority of

1026 our framework in the challenging task of simultaneous and coherent audio-video synthesis from a
 1027 shared latent space.
 1028

1029

1030

1031 **Overall Conclusion from User Study** The user study provides a clear and compelling validation
 1032 of our unified framework. Ours distinguishes itself not as a master of one trade, but as a master
 1033 of a far more complex one: multi-modal coherence. It establishes state-of-the-art performance in
 1034 simultaneous audio-video generation, demonstrates a critical and superior capability in A2V reference
 1035 consistency, and is highly competitive in TTS text alignment. While unimodal expert models lead
 1036 in their narrow domains, our model’s success across the most challenging joint and directional
 1037 tasks proves that our approach effectively pioneers a versatile, powerful, and efficient paradigm for
 1038 open-source audio-video joint generation.
 1039

1040

1041

G QWEN2.5-OMNI PROMPT USED IN DATA PIPELINE

1042

1043

1044

Prompt1

1045

1046

1047

You are a video marking expert responsible for labeling the provided video and audio and outputting JSON. The main labels include:

1. The overall detailed style description of the video, such as realistic, abstract, cartoon, freehand, 1960s, etc.
2. Characters appearing in the video or well-known IPs (Iron Man, Minions, etc.), with detailed appearance descriptions, such as a man wearing a black suit, a white shirt inside the suit, a red tie, and black narrow-framed glasses, etc.
3. Objects appearing in the video, with detailed appearance descriptions, such as a football with white, red, and blue stripes in the lower left corner.
4. Interactions between characters and objects or between characters, such as a man walking towards the football and trying to pad it.
5. Background description of the video, such as a light blue sea in the background, a white beach in front, and some colorful balloons scattered on the beach.
6. Character role in the video and their speech content, such as [the man saying: 'Today we are going to learn beach football, which is completely different from beach volleyball.']}
7. Dynamic description of events in the video, such as when the man lifts the football with his foot, the football is kicked high and flies to the right of the screen, the screen moves to the right with the football, and the football falls into the basket on the beach.
8. Ambient sounds in the video, such as the sound of seagulls, the whistle of ships, the sound of waves.
9. Comprehensive description, objectively and detailedly describing the content of the video, emphasizing the main content of the video, and describing the character movements, camera switching methods, background environment, ambient sounds and speech content in the video audio, etc.

1075

1076

1077

1078

1079

Instruction: You should first infer how many speakers are in the video implicitly, then identify which character said what content accurately according to video lip movement and corresponding audio speech; use the ASR results as a reference for speech content recognition.

1080
1081

prompt2

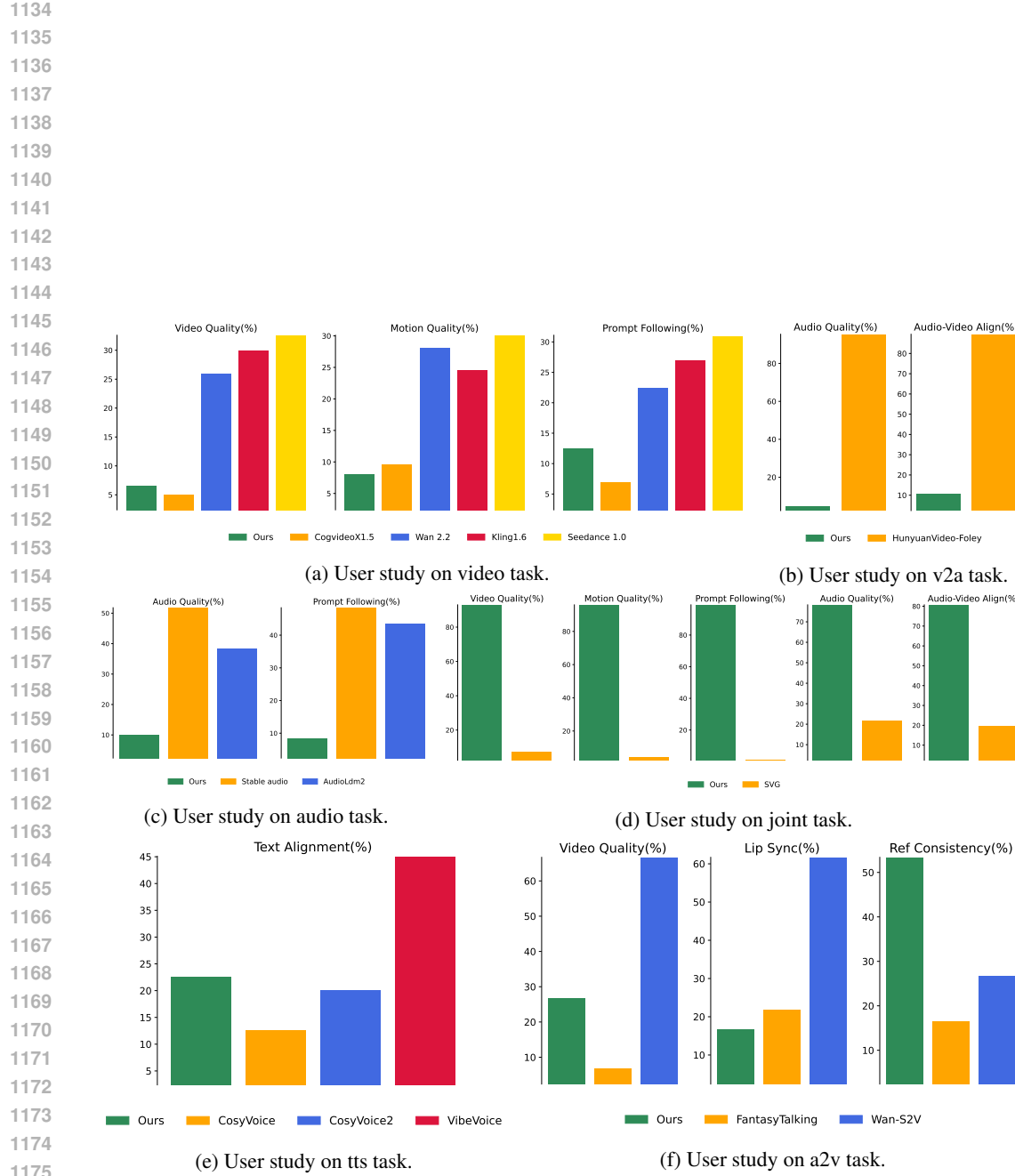
1082 [Output requirements]: The above content is used as a basic unit,
1083 and multiple unit contents are described cyclically as the video
1084 progresses. Each item in the output dict should include a detailed
1085 description respectively, and the content is output in JSON format.
1086 The basic format is as follows:

1087 -----Example Start-----

```

1088 {
1089     "Video Style": "xxx",
1090     "Unit 1": {
1091         "Character": ["xxx", "xxx"],
1092         "Character descriptions": ["xxx", "xxx"],
1093         "Object": ["xxx", "xxx", "xxx"],
1094         "Character Interaction": "xxx",
1095         "Background Description": "xxx",
1096         "Speech Content": ["xxx", "xxx"],
1097         "Event Dynamic Description": "xxx",
1098         "Ambient Sound": ["xxx", "xxx"],
1099         "Comprehensive Description": "xxx"
1100     },
1101     ...
1102     "Unit n": {
1103         ...
1104     },
1105 }
1106 -----Example End-----
```

1103 [Note]: Please fill in the above content according to the video
1104 content, ignore the possible subtitles in the video. The output
1105 format is JSON.1107 The complete prompt to Qwen2.5-Omni is $Prompt_1 + transcript + Prompt_2$. Where $transcript$
1108 is the tts results from Whisper.1109
1110
1111
1112
1113
1114
1115
1116
1117
1118
1119
1120
1121
1122
1123
1124
1125
1126
1127
1128
1129
1130
1131
1132
1133

Figure 4: User study of our method with baseline methods. Best viewed with **zoom-in**.

1188
1189
1190
1191
1192
1193
1194
1195
1196
1197
1198
1199

1200
1201

Table 3: Detailed Audio Classification Statistics for Set 1

Category / Subcategory	Count	Percentage (%)
Natural Environment	70	36.3
Weather-Wind	18	
Plants-Vegetation	12	
Animals-Birds	10	
Water-Ocean/Waves	8	
<i>Other Natural Subcategories</i>	22	
Music & Instruments	40	20.7
Musical Compositions	14	
Keyboard-Piano	7	
String-Guitar	7	
<i>Other Music Subcategories</i>	12	
Daily Life	22	11.4
Office-Writing/Typing	4	
Tools-Electronics	4	
<i>Other Daily Life Subcategories</i>	14	
Human Voices	21	10.9
Adults-Conversation	6	
<i>Other Human Voices Subcategories</i>	15	
Transportation	12	6.2
Industrial & Urban	10	5.2
Special Effects	9	4.7
Weapons & Explosions	7	3.6
Total Classified	191	93.2
Unclassified	14	6.8
Grand Total	205	100.0

1229
1230
1231
1232
1233
1234
1235
1236
1237
1238
1239
1240
1241

1242
1243
1244
1245
1246
1247
1248
1249
1250
1251
1252
1253
1254

Table 4: Detailed Audio Classification Statistics for Set 2

Category / Subcategory	Count	Percentage (%)
Natural Environment	106	35.9
Weather-Wind	22	
Animals-Birds	22	
Weather-Rain	19	
Animals-Dogs	9	
<i>Other Natural Subcategories</i>	34	
Music & Instruments	54	18.3
Musical Compositions	16	
Keyboard-Piano	10	
String-Violin	8	
<i>Other Music Subcategories</i>	20	
Daily Life	28	9.5
Office-Writing/Typing	6	
Tools-Power Tools	6	
Communication-Phone	6	
<i>Other Daily Life Subcategories</i>	10	
Human Voices	16	5.4
Adults-Conversation	9	
<i>Other Human Voices Subcategories</i>	7	
Transportation	10	3.4
Industrial & Urban	9	3.1
Weapons & Explosions	5	1.7
Special Effects	2	0.7
Total Classified	230	78.0
Unclassified	65	22.0
Grand Total	295	100.0

1285
1286
1287
1288
1289
1290
1291
1292
1293
1294
1295

1296
 1297
 1298
 1299
 1300
 1301
 1302
 1303
 1304
 1305
 1306
 1307

Table 5: Combined Audio Classification Statistics for Set 1 & Set 2

Category / Subcategory	Count	Percentage (%)
Natural Environment	176	36.1
Weather-Wind	40	
Animals-Birds	32	
Weather-Rain	23	
Plants-Vegetation	15	
<i>Other Natural Subcategories</i>	66	
Music & Instruments	94	19.3
Musical Compositions	30	
Keyboard-Piano	17	
String-Guitar	13	
String-Violin	12	
<i>Other Music Subcategories</i>	22	
Daily Life	50	10.2
Office-Writing/Typing	10	
Tools-Power Tools	8	
<i>Other Daily Life Subcategories</i>	32	
Human Voices	37	7.6
Adults-Conversation	15	
<i>Other Human Voices Subcategories</i>	22	
Transportation	22	4.5
Vehicles-Cars	19	
Industrial & Urban	19	3.9
Fire & Combustion	14	
Weapons & Explosions	12	2.5
Special Effects	11	2.3
Total Classified	421	84.2
Unclassified	79	15.8
Grand Total	500	100.0

1340
 1341
 1342
 1343
 1344
 1345
 1346
 1347
 1348
 1349

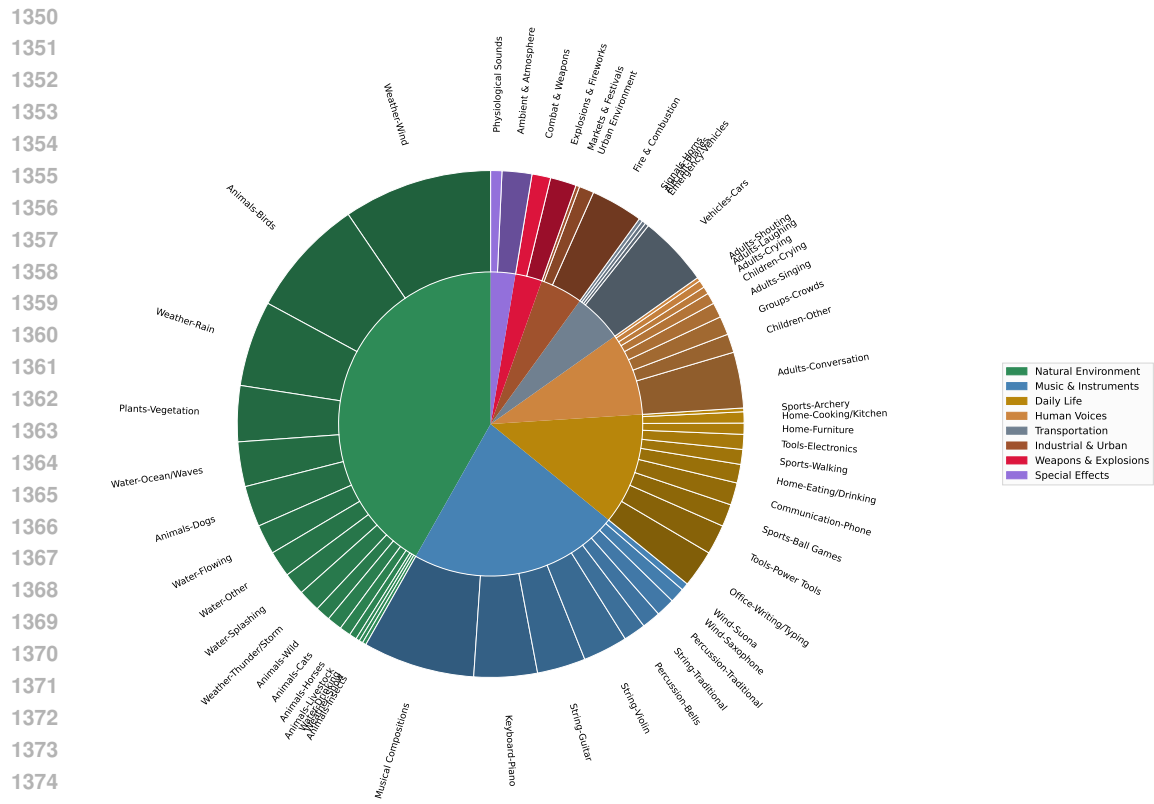


Figure 5: Statistical results of set1 and 2.

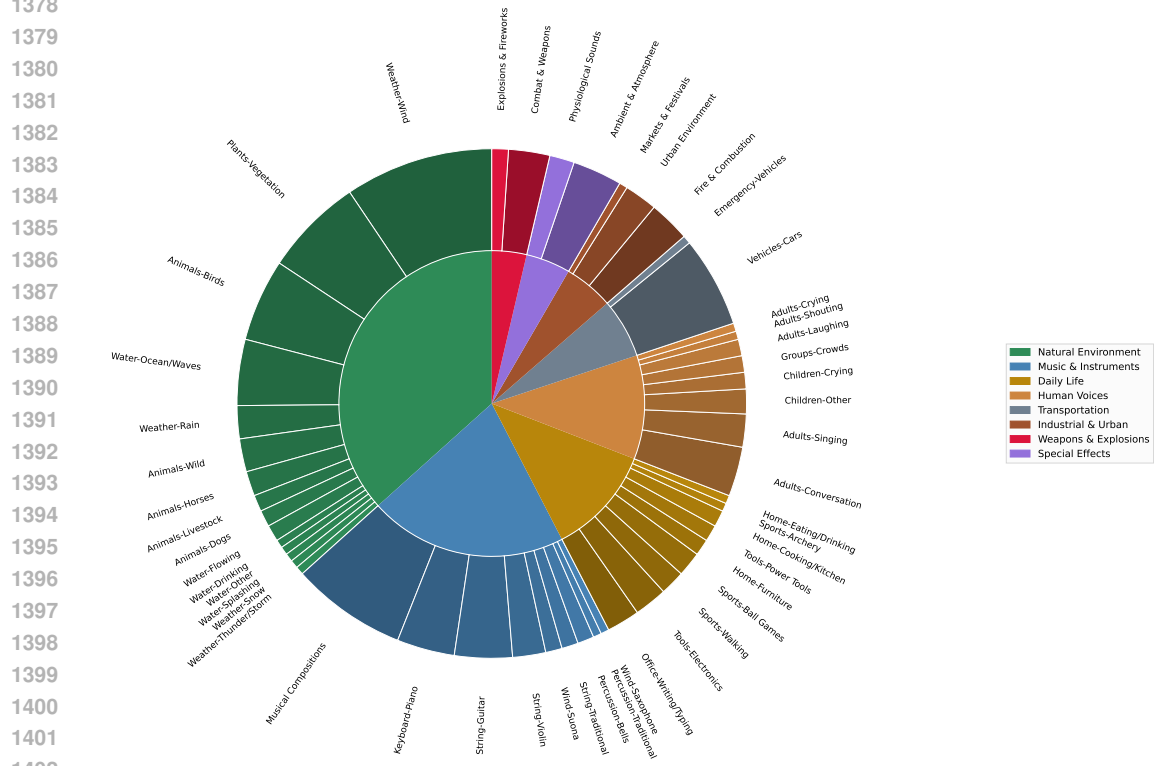


Figure 6: Statistical results of set1.

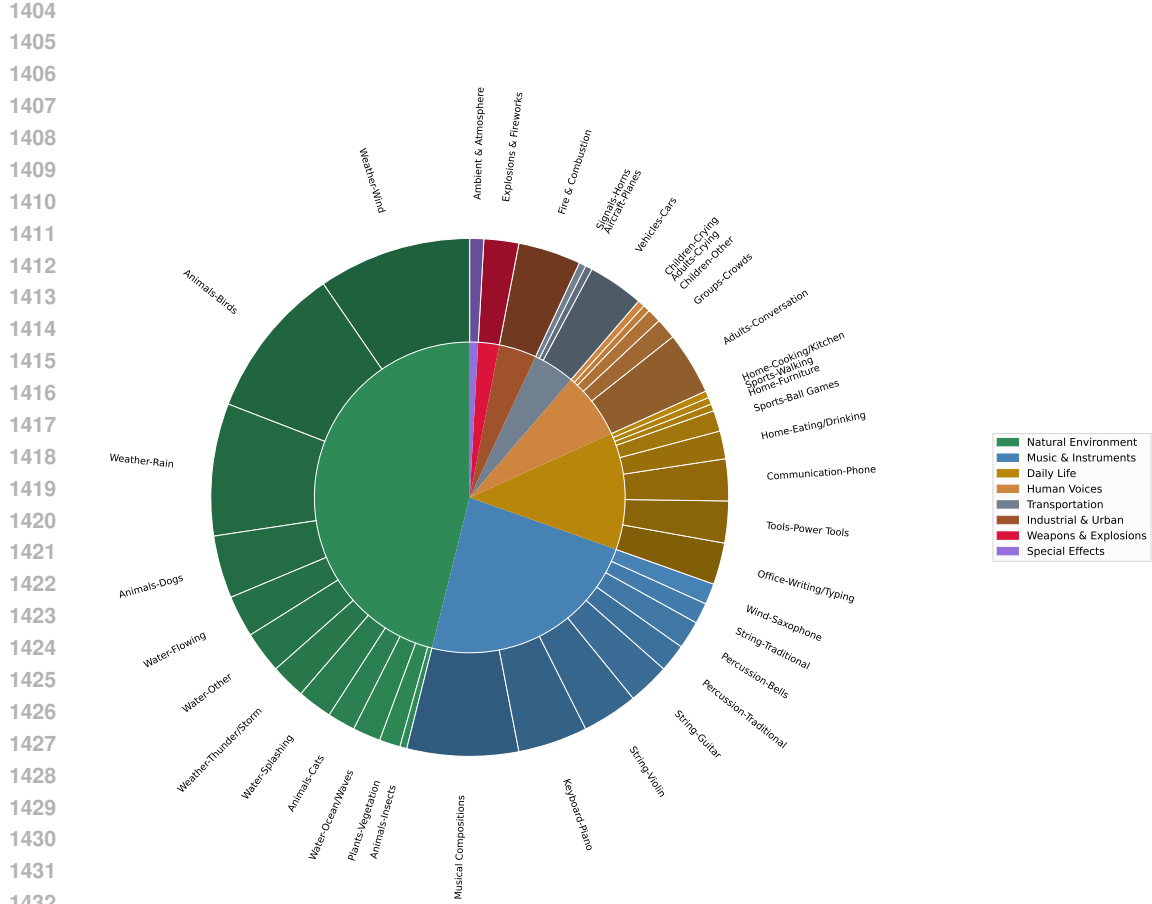


Figure 7: Statistical results of set2.

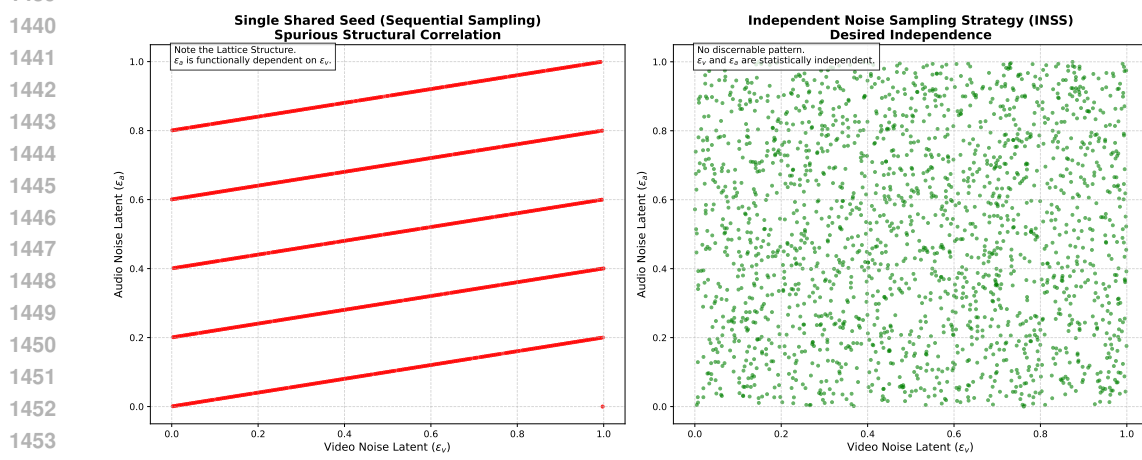


Figure 8: Visualization of effectiveness of INSS in a sample data space.